

Introduction to sparse-data X-ray tomography: Part A

Samuli Siltanen

Department of Mathematics and Statistics
University of Helsinki, Finland
samuli.siltanen@helsinki.fi
www.siltanen-research.net

IMPA, Rio de Janeiro, Brazil

Symposium on Inverse Problems in Science and Engineering
October 24–27, 2017





Finnish Centre of Excellence in Inverse Problems Research





Finnish Centre of Excellence in Inverse Modelling and Imaging



UNIVERSITY OF JYVÄSKYLÄ



TAMPERE UNIVERSITY OF TECHNOLOGY



FINNISH METEOROLOGICAL INSTITUTE



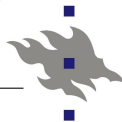
Finland



UNIVERSITY OF
EASTERN FINLAND



LUT
Lappeenranta
University of Technology



UNIVERSITY OF HELSINKI



Aalto University

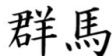
This my industrial-academic background



1999: PhD, Helsinki University of Technology, Finland



2000: R&D scientist at Instrumentarium Imaging



2002: Postdoc at Gunma University, Japan



2004: R&D scientist at GE Healthcare



2005: R&D scientist at Palodex Group



2006: Professor, Tampere University of Technology, Finland



2009: Professor, University of Helsinki, Finland

Course team

Markus Juvonen

Alexander Meaney

Lotus root tomography

YouTube search: "lotus tomography"

www.youtube.com/watch?v=eWwD_EZuzBI&t=7s

Video: thanks to Tatiana Bubba, Andreas Hauptmann and Juho Rimpeläinen

Outline

X-ray tomography

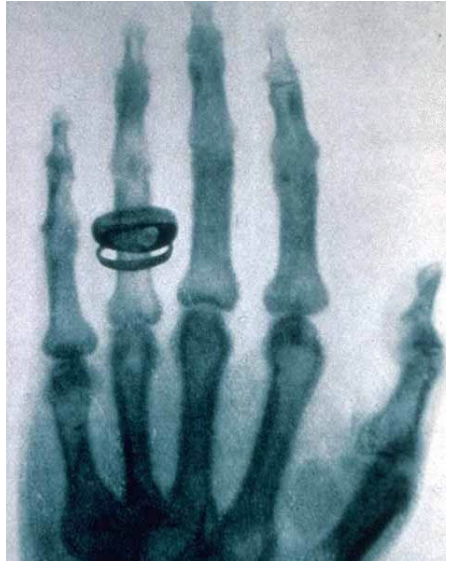
Mathematical model of X-ray attenuation

Tomography with few data: ill-posed inverse problem

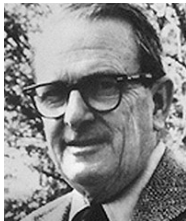
Regularized inversion

A real-world example

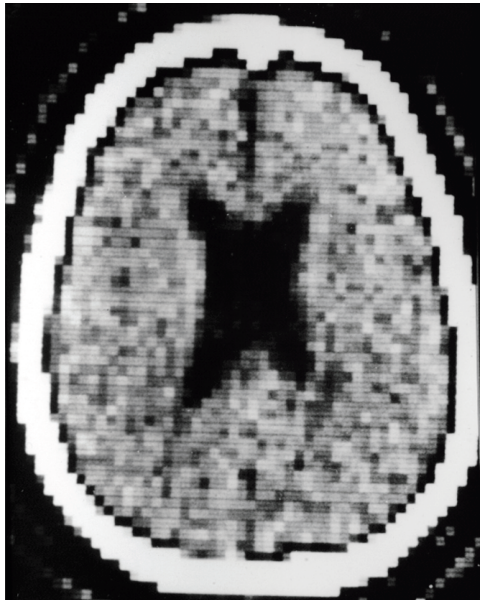
Wilhelm Conrad Röntgen invented X-rays and was awarded the first Nobel Prize in Physics in 1901



Godfrey Hounsfield and Allan McLeod Cormack developed X-ray tomography



Hounsfield (top) and Cormack received Nobel prizes in 1979.



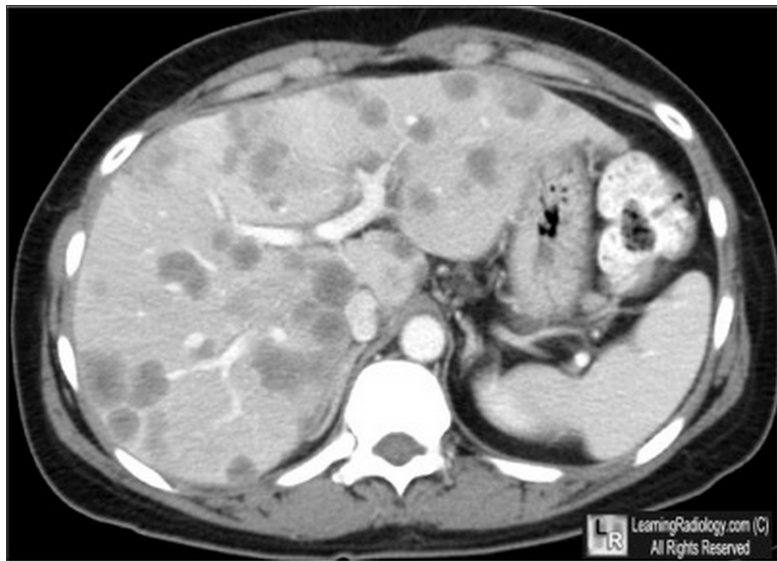
Reconstruction of a function from its line integrals
was first invented by Johann Radon in 1917



Johann Radon (1887-1956)

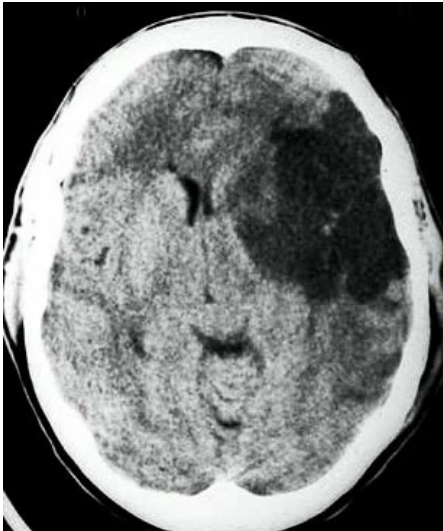
$$f(P) = -\frac{1}{\pi} \int_0^{\infty} \frac{d\overline{F}_p(q)}{q}$$

Contrast-enhanced CT of abdomen, showing liver metastases



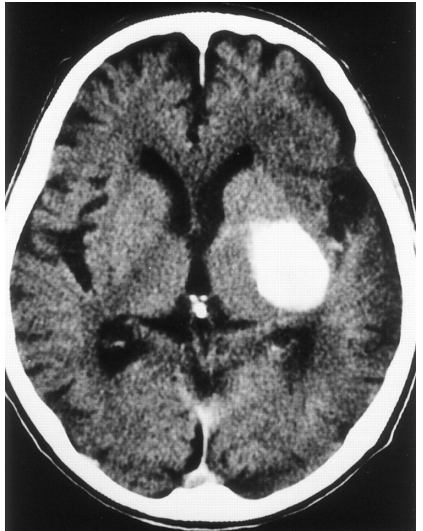
Diagnosing stroke with X-ray tomography

Ischemic stroke



CT image from Jansen 2008

Hemorrhagic stroke



CT image from Nakano *et al.* 2001

Unusual variant of the Nutcracker Fracture of the calcaneus and tarsal navicular



[Gajendran, Yoo & Hunter, Radiology Case Reports 3 (2008)]

Outline

X-ray tomography

Mathematical model of X-ray attenuation

Tomography with few data: ill-posed inverse problem

Regularized inversion

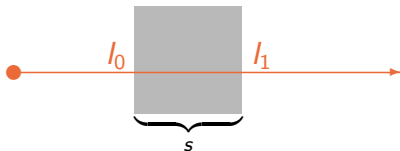
A real-world example

**X-ray intensity attenuates inside matter,
here shown with a homogeneous block**

<https://www.youtube.com/watch?v=IfXo2S1xXCQ>

Formula for X-ray attenuation along a line inside homogeneous matter

An X-ray with intensity I_0 enters a homogeneous physical body.



The intensity I_1 of the X-ray when it exits the material is

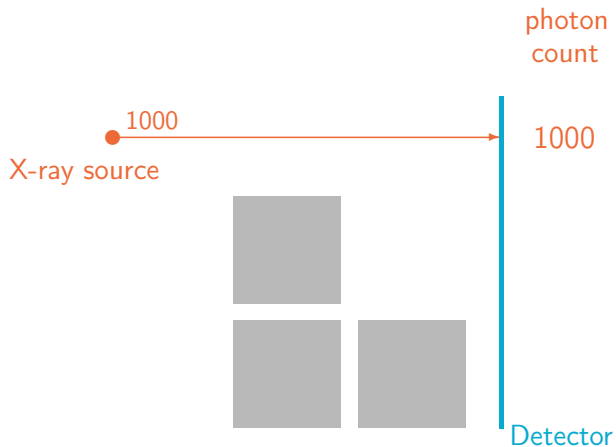
$$I_1 = I_0 e^{-\mu s},$$

where s is the length of the path of the X-ray inside the body and $\mu > 0$ is X-ray attenuation coefficient.

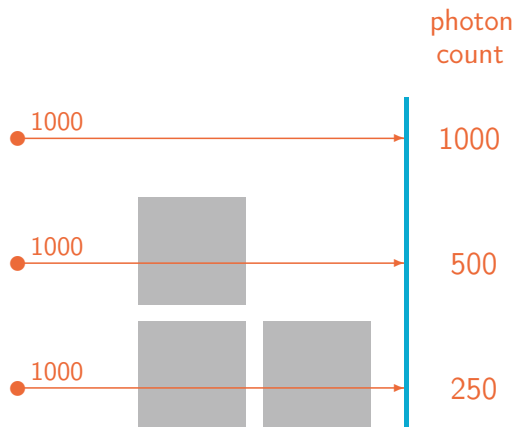
**X-ray intensity attenuates inside matter,
here shown with two homogeneous blocks**

https://www.youtube.com/watch?v=Z_IBFQcn0l8

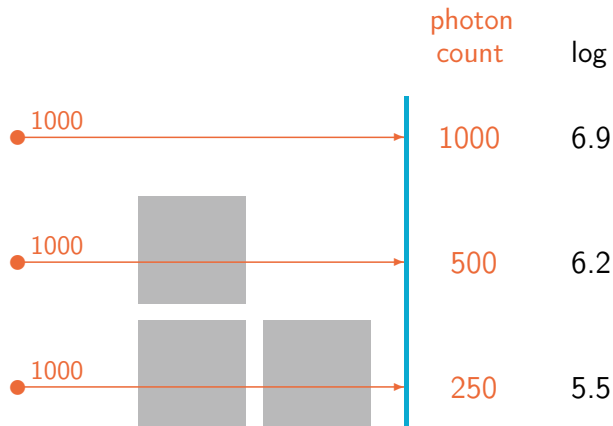
A digital X-ray detector counts how many photons arrive at each pixel



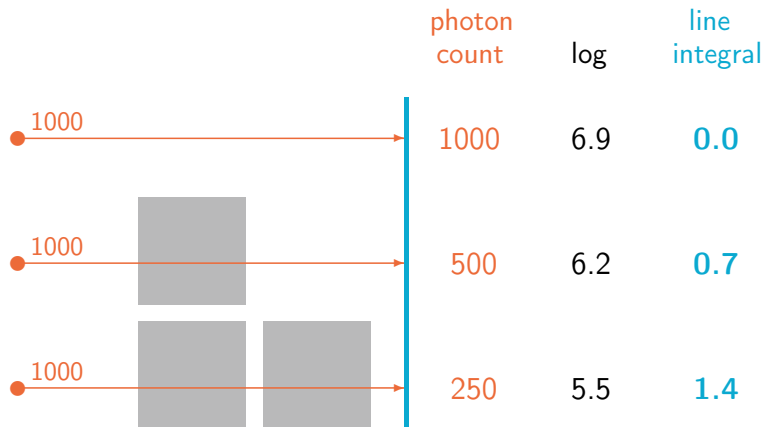
Adding material between the source and detector reveals the exponential X-ray attenuation law



We take logarithm of the photon counts to compensate for the exponential attenuation law



Final calibration step is to subtract the logarithms from the empty space value (here 6.9)



Formula for X-ray attenuation along a line: Beer-Lambert law

Let $f : [a, b] \rightarrow \mathbb{R}$ be a nonnegative function modelling X-ray attenuation along a line inside a physical body.

Beer-Lambert law connects the initial and final intensities:

$$I_1 = I_0 e^{-\int_a^b f(x) dx}.$$

We can also write it in the form

$$-\log(I_1/I_0) = \int_a^b f(x) dx,$$

where I_0 is known from calibration and I_1 from measurement.

After calibration we are observing how much attenuating matter the X-ray encounters

<https://www.youtube.com/watch?v=TKqcrDGPsAI>

This sweeping movement is the data collection mode of first-generation CT scanners

<https://www.youtube.com/watch?v=TbLaQo3rgEE>

Rotating around the object allows us to form
the so-called *sinogram*

<https://www.youtube.com/watch?v=5Vyc1TzmNI8>

Modern CT scanners look like this



Modern scanners rotate at high speed

Hellerhoff & Markwitz, Wikimedia commons

**This is an illustration of the standard
reconstruction by filtered back-projection**

Outline

X-ray tomography

Mathematical model of X-ray attenuation

Tomography with few data: ill-posed inverse problem

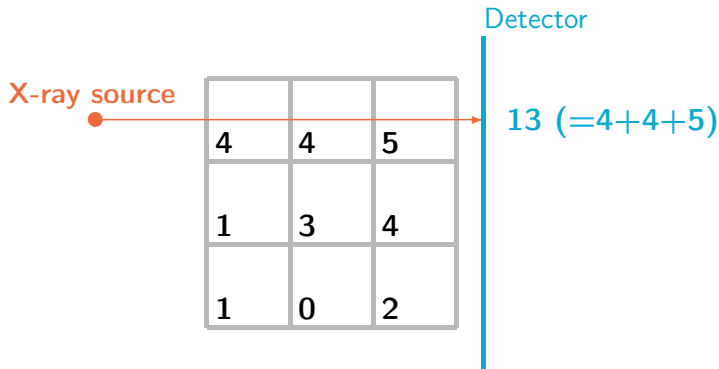
Regularized inversion

A real-world example

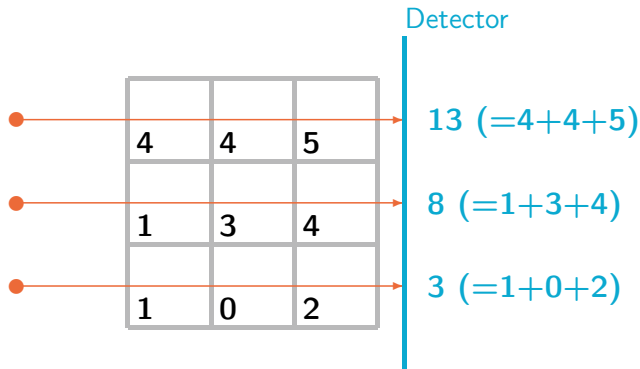
Let us study a simple two-dimensional example of tomographic imaging

4	4	5
1	3	4
1	0	2

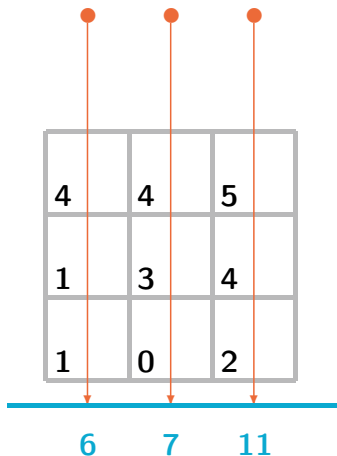
Tomography is based on measuring densities of matter using X-ray attenuation data



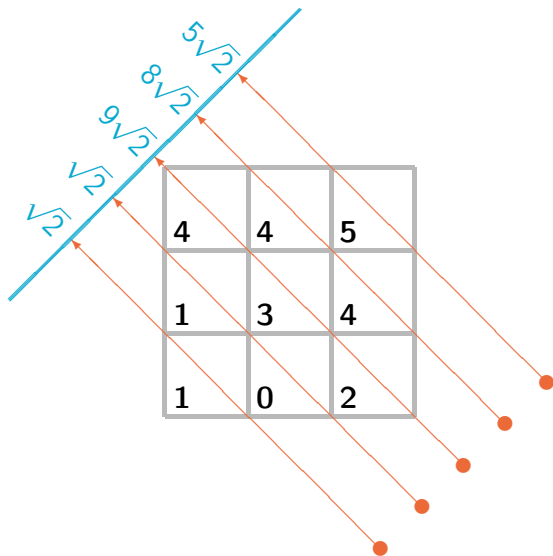
A projection image is produced by parallel X-rays and several detector pixels (here three pixels)



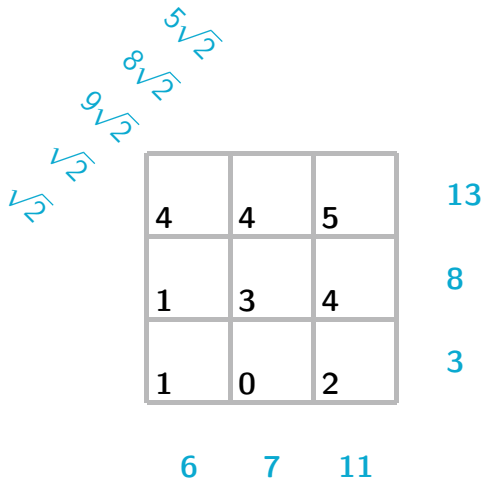
For tomographic imaging it is essential to record projection images from different directions



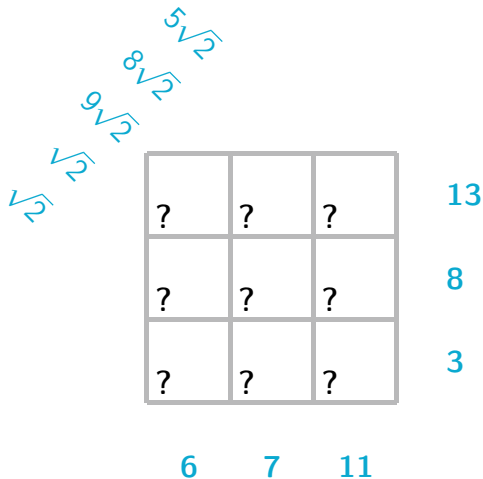
The length of X-rays traveling inside each pixel is important, thus here the square roots



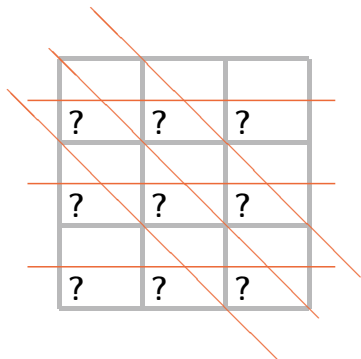
The direct problem of tomography is to find the projection images from known tissue



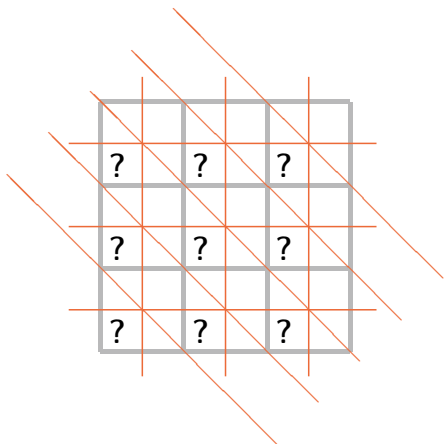
The inverse problem of tomography is to reconstruct the interior from X-ray data



The limited-angle problem is harder than the full-angle problem

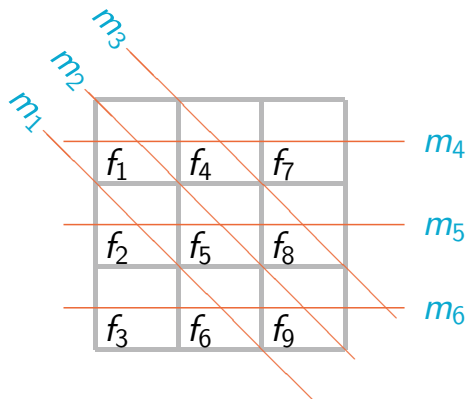


9 unknowns,
6 equations



9 unknowns,
11 equations

We write the reconstruction problem
in matrix form

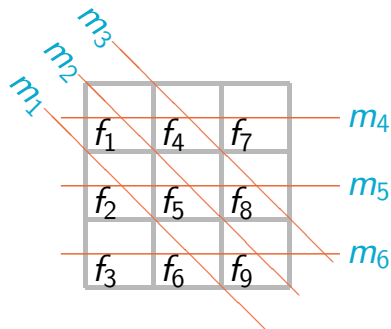


$$f = \begin{bmatrix} f_1 \\ f_2 \\ f_3 \\ f_4 \\ f_5 \\ f_6 \\ f_7 \\ f_8 \\ f_9 \end{bmatrix}, \quad m = \begin{bmatrix} m_1 \\ m_2 \\ m_3 \\ m_4 \\ m_5 \\ m_6 \end{bmatrix},$$

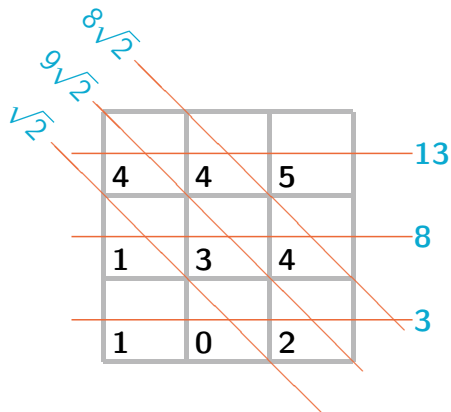
Measurement model: $m = Af + \varepsilon$

This is the matrix equation related to the above measurement

$$\begin{bmatrix} m_1 \\ m_2 \\ m_3 \\ m_4 \\ m_5 \\ m_6 \end{bmatrix} = \begin{bmatrix} 0 & \sqrt{2} & 0 & 0 & 0 & \sqrt{2} & 0 & 0 & 0 \\ \sqrt{2} & 0 & 0 & 0 & \sqrt{2} & 0 & 0 & 0 & \sqrt{2} \\ 0 & 0 & 0 & \sqrt{2} & 0 & 0 & 0 & \sqrt{2} & 0 \\ 1 & 0 & 0 & 1 & 0 & 0 & 1 & 0 & 0 \\ 0 & 1 & 0 & 0 & 1 & 0 & 0 & 1 & 0 \\ 0 & 0 & 1 & 0 & 0 & 1 & 0 & 0 & 1 \end{bmatrix} \begin{bmatrix} f_1 \\ f_2 \\ f_3 \\ f_4 \\ f_5 \\ f_6 \\ f_7 \\ f_8 \\ f_9 \end{bmatrix} + \begin{bmatrix} \varepsilon_1 \\ \varepsilon_2 \\ \varepsilon_3 \\ \varepsilon_4 \\ \varepsilon_5 \\ \varepsilon_6 \end{bmatrix}$$



In limited-angle imaging, different objects may produce the same data



5	6	2
1	5	2
4	0	-1

9	1	3
1	0	7
3	0	0

Mathematically this means that the matrix A has nontrivial kernel.

We can solve the limited-angle problem using minimum norm solution

Consider the matrix equation $Af = m$, where $f \in \mathbb{R}^n$ and $m \in \mathbb{R}^k$ and A has size $k \times n$.

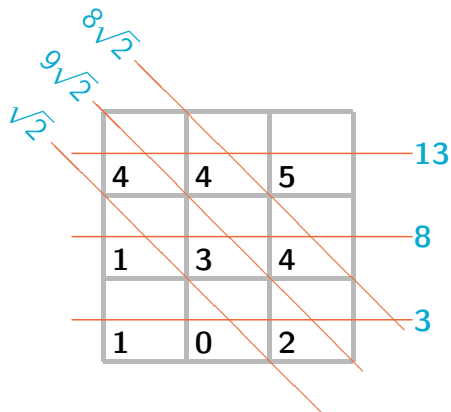
Definition. A vector $\tilde{f} \in \mathbb{R}^n$ is called a *least-squares solution* of the equation $Af = m$ if

$$\|A\tilde{f} - m\| = \min_{z \in \mathbb{R}^n} \|Az - m\|.$$

Furthermore, \tilde{f} is called the *minimum norm solution* if

$$\|\tilde{f}\| = \inf\{\|z\| : z \text{ is a least-squares solution of } Af = m\}.$$

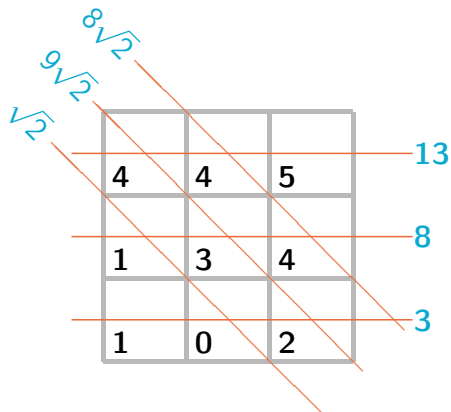
This is the minimum norm solution for our limited-angle case



Minimum norm solution

5	8	0
8	0	0
6	-7	4

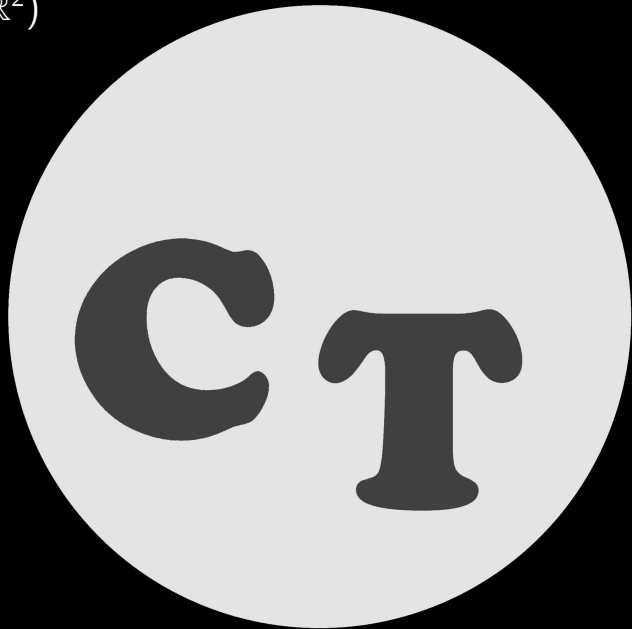
This is the non-negative minimum norm solution for our limited-angle case



Non-negative
minimum norm
solution

9	0	4
0	0	8
2	1	0

Let us construct a more complicated example,
first in $L^2(\mathbb{R}^2)$



Let us construct a more complicated example,
first in $L^2(\mathbb{R}^2)$

$$f = 0.44$$



0.16

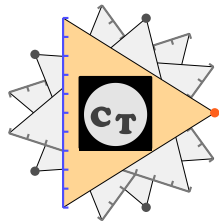


0.16

$$f = 0$$

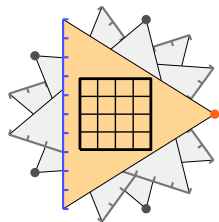
The continuous tomographic model needs to be approximated using a discrete model

Continuous model:



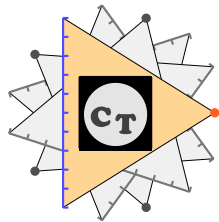
In this schematic setup we have 5 projection directions and a 10-pixel detector. Therefore, the number of data points is **50**.

Discrete model:



The resolution of the discrete model can be freely chosen according to computational resources

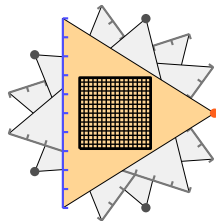
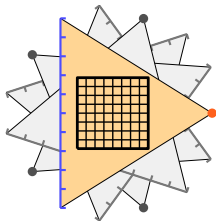
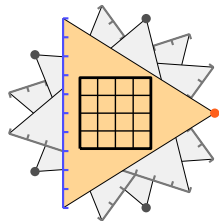
Continuous model:



In this schematic setup we have 5 projection directions and a 10-pixel detector. Therefore, the number of data points is **50**.

The number of degrees of freedom in the three discrete models below are **16**, **64** and **256**, respectively.

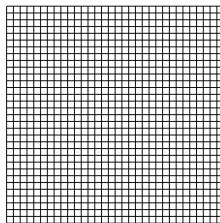
Discrete models:



Discretize the unknown by dividing it into pixels



Target (unknown)

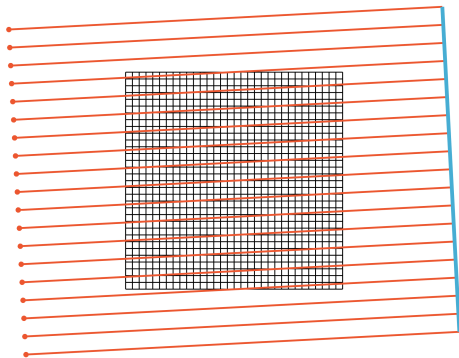


32×32 pixel grid

System matrix A , given by the grid and X-rays

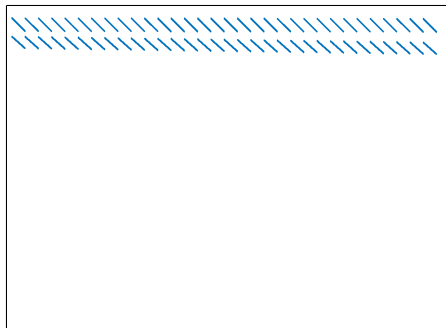


735×1024 system matrix A ,
only nonzero elements shown

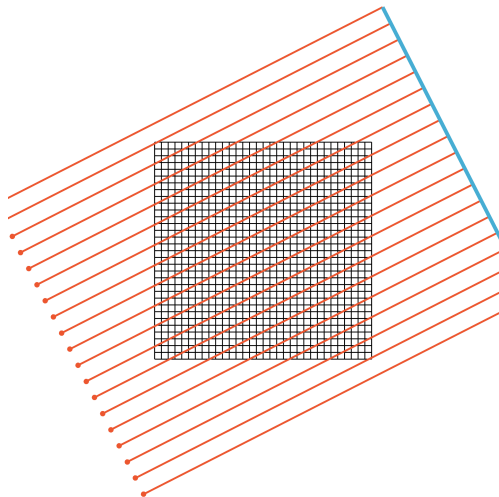


32×32 pixel grid

System matrix A , given by the grid and X-rays

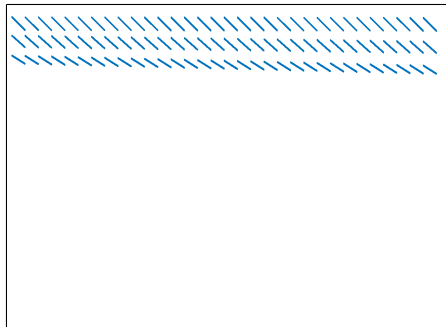


735×1024 system matrix A ,
only nonzero elements shown

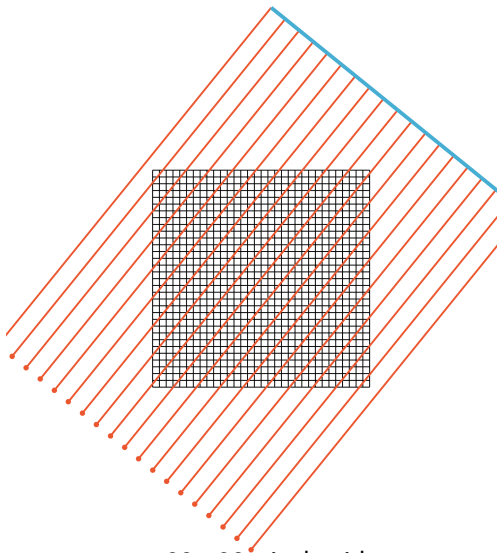


32×32 pixel grid

System matrix A , given by the grid and X-rays

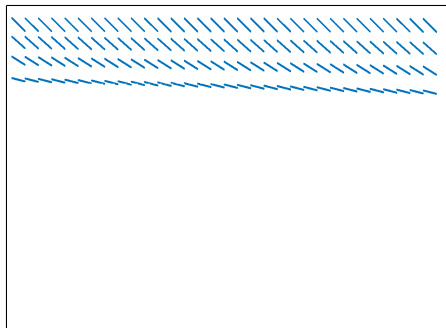


735×1024 system matrix A ,
only nonzero elements shown

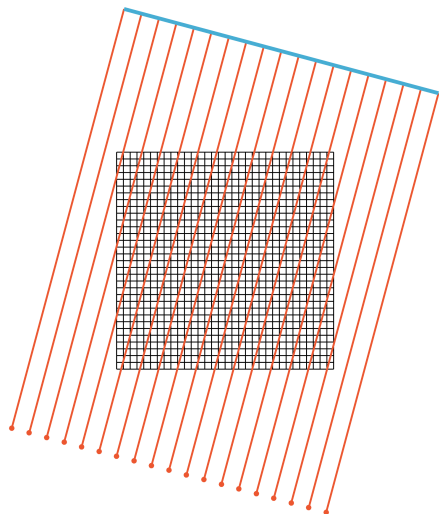


32×32 pixel grid

System matrix A , given by the grid and X-rays

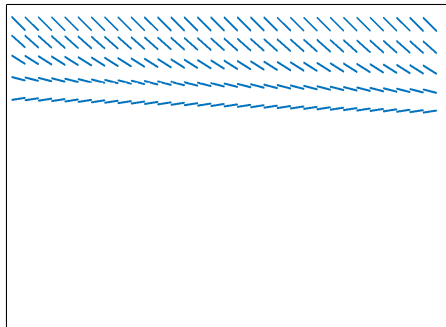


735×1024 system matrix A ,
only nonzero elements shown

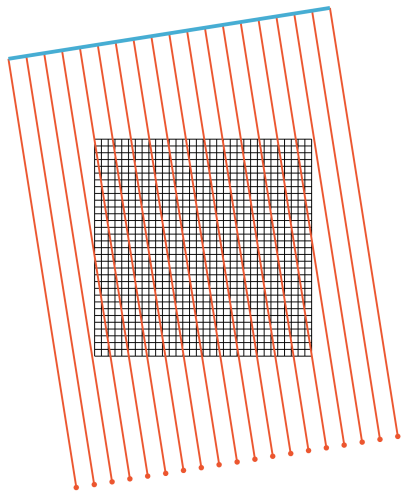


32×32 pixel grid

System matrix A , given by the grid and X-rays

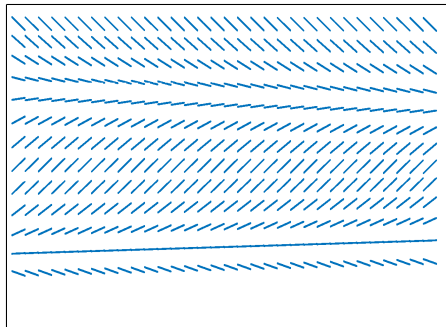


735×1024 system matrix A ,
only nonzero elements shown

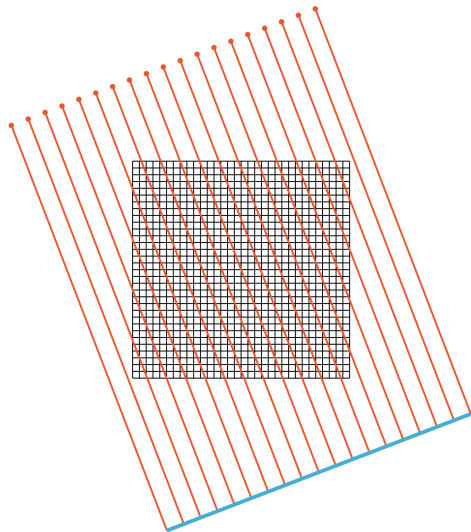


32×32 pixel grid

System matrix A , given by the grid and X-rays

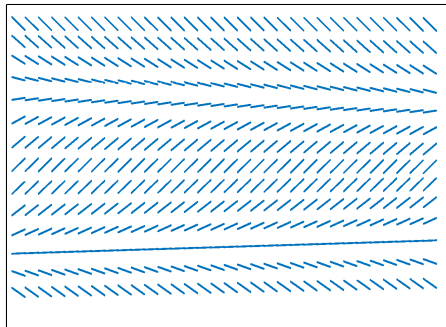


735×1024 system matrix A ,
only nonzero elements shown

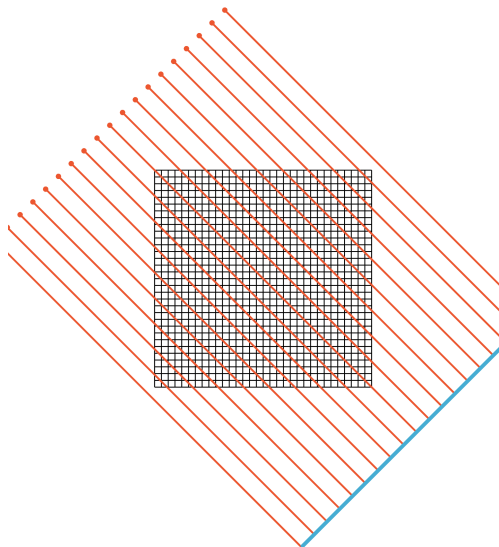


32×32 pixel grid

System matrix A , given by the grid and X-rays

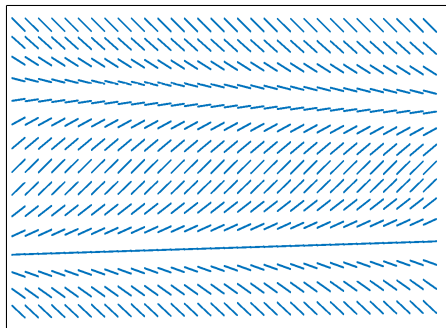


735×1024 system matrix A ,
only nonzero elements shown

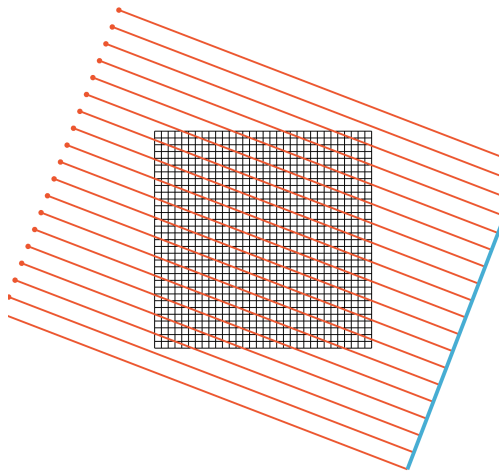


32×32 pixel grid

System matrix A , given by the grid and X-rays



735×1024 system matrix A ,
only nonzero elements shown

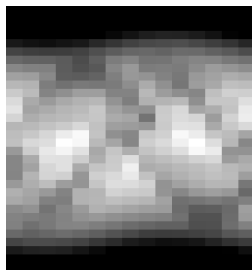
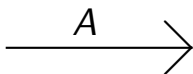


32×32 pixel grid

What can we expect to see from sparse data?



Object



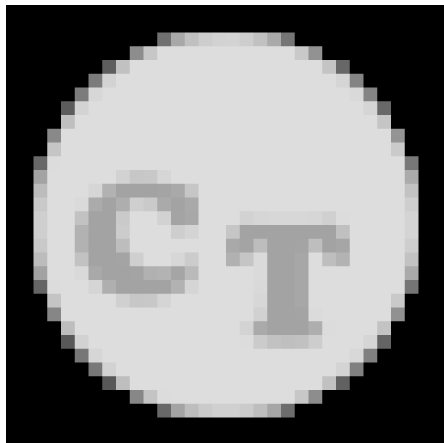
Sinogram

THEOREM 4.2. *A finite set of radiographs tells nothing at all.*

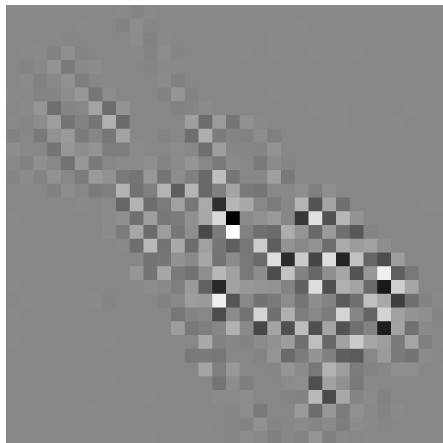
For some reason this theorem provokes merriment. It is so plainly one of those mathematical ideals untainted by any possibility of practical application.

[Cormack 1963], [Smith, Solmon & Wagner 1977, Theorem 4.2]

Naive reconstruction using the minimum norm solution $(A^T A)^{-1} A^T m$



Original phantom, values between zero (black) and 0.44

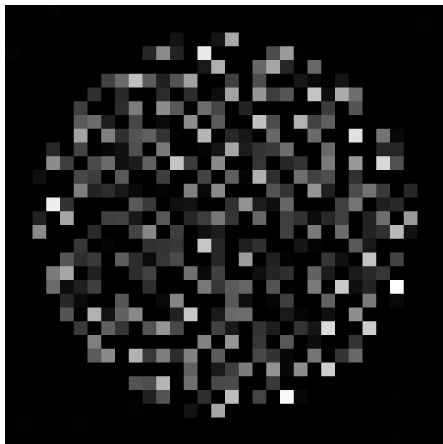


Reconstruction: minimum pixel value $-1.5 \cdot 10^{14}$, maximum value $1.3 \cdot 10^{14}$

Naive reconstruction using the minimum norm solution with non-negativity constraint

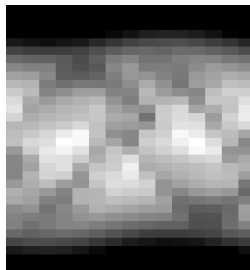
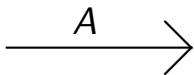


Original phantom, values between zero (black) and 0.44



Reconstruction: minimum value 0, maximum value 2.3

Illustration of the ill-posedness of sparse tomography



Difference 0.00992

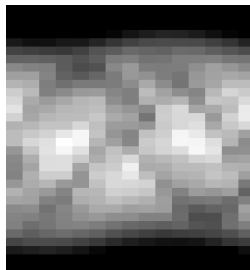
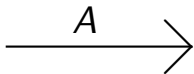
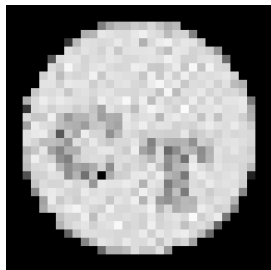
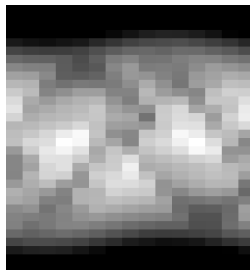
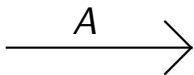
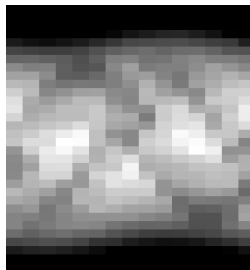
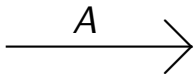
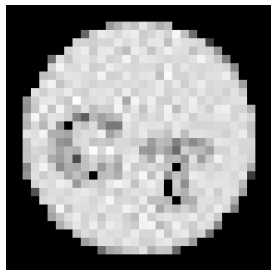


Illustration of the ill-posedness of sparse tomography



Difference 0.00983



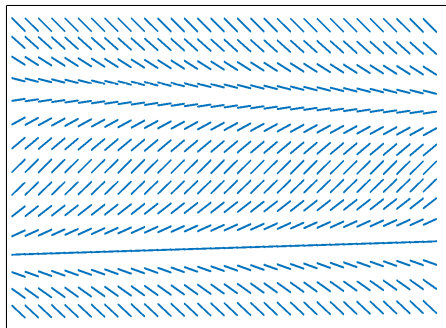
Singular Value Decomposition for $k \times n$ matrix A :
 $A = UDV^T$ with $UU^T = I = U^T U$ and $VV^T = I = V^T V$

$$A = UDV^T = U \begin{bmatrix} d_1 & 0 & \cdots & 0 & \cdots & 0 \\ 0 & d_2 & & & & \vdots \\ \vdots & & \ddots & & & \\ & & & d_r & & \\ & & & & 0 & \\ \vdots & & & & & \ddots \\ 0 & \cdots & & & & \cdots & 0 \end{bmatrix} V^T$$

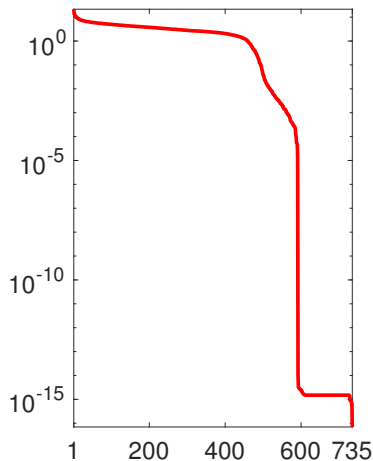
The singular values d_j satisfy $d_1 \geq d_2 \geq \cdots \geq d_r > 0$
and $d_{r+1} = d_{r+2} = \cdots = d_{\min\{k,n\}} = 0$. Note that $r = \text{rank}(A)$.

If $n = k$ and all singular values are positive, then A is invertible.
However, the *condition number* $\text{cond}(A) := d_1/d_r$ may be large.
In that case A^{-1} is a numerically unstable matrix.

Singular value decomposition $A = U^T D V$

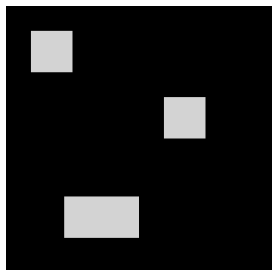


735 \times 1024 system matrix A ,
only nonzero elements shown

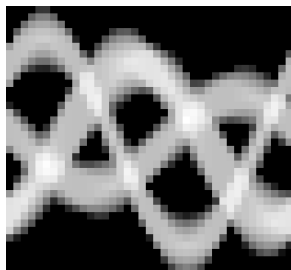
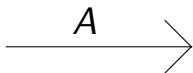


Singular values of A
(diagonal of D)

We have object and data for the inverse problem

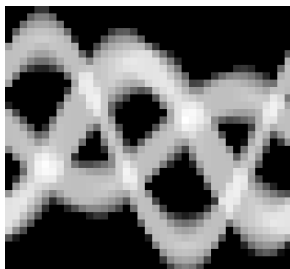
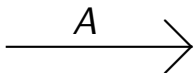
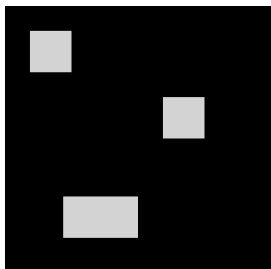


$$f \in \mathbb{R}^{32 \times 32}$$



$$Af \in \mathbb{R}^{49 \times 39}$$

Illustration of the ill-posedness of tomography



Difference 0.00254

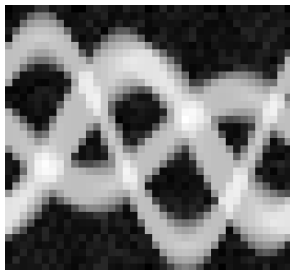
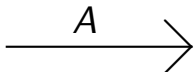
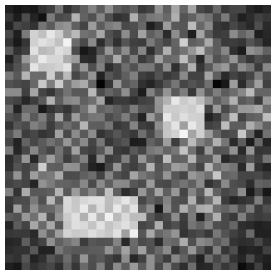
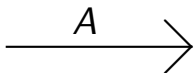
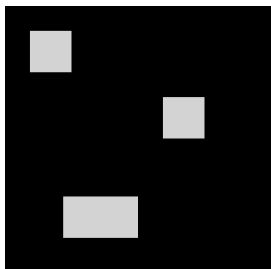


Illustration of the ill-posedness of tomography



Difference 0.00124

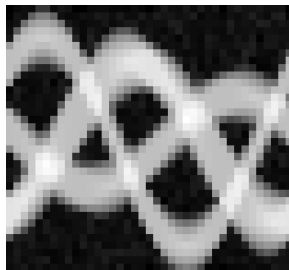
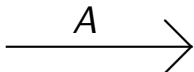
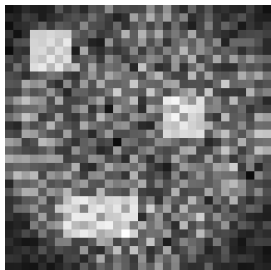
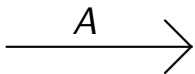
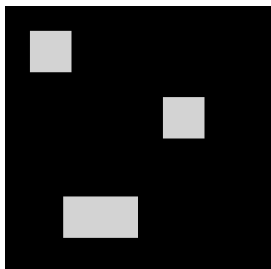
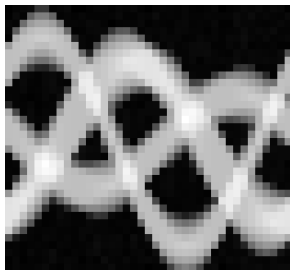
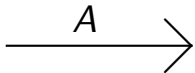
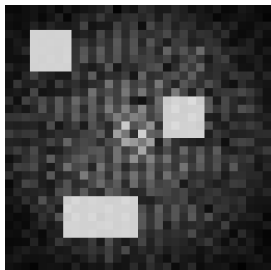


Illustration of the ill-posedness of tomography



Difference 0.00004



Outline

X-ray tomography

Mathematical model of X-ray attenuation

Tomography with few data: ill-posed inverse problem

Regularized inversion

A real-world example

Recall Hadamard's conditions for a well-posed problem



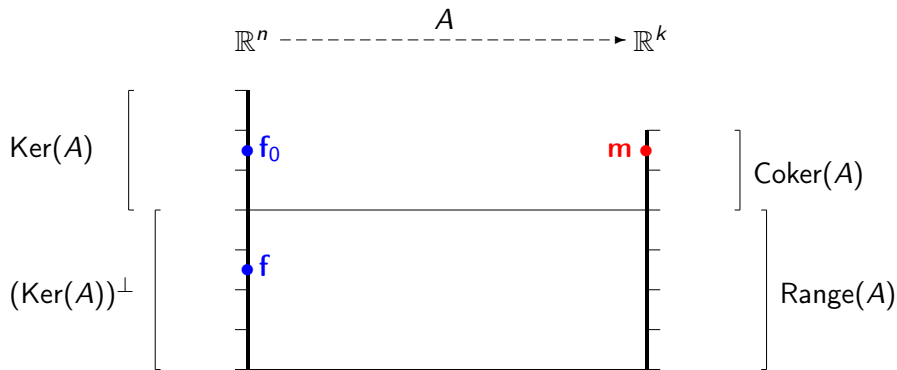
Hadamard (1903): a problem is well-posed if the following conditions hold.

1. A solution exists,
2. The solution is unique,
3. The solution depends continuously on the input.

Ill-posed inverse problem:

Input noisy data $m = Af + \varepsilon$, recover f .

Hadamard's conditions in a linear inverse problem with forward map given by a matrix A



The matrix A maps bijectively between $(\text{Ker}(A))^\perp$ and $\text{Range}(A)$. However, decreasing singular values may make this bijection unstable, leading to trouble with Hadamard's condition 3.

The Moore-Penrose pseudoinverse takes care of Hadamard's conditions 1 and 2

$$A^\dagger = VD^\dagger U^T = V \begin{bmatrix} 1/d_1 & 0 & \cdots & 0 & \cdots & 0 \\ 0 & 1/d_2 & & & & \vdots \\ \vdots & & \ddots & & & \\ & & & 1/d_r & & \\ & & & & 0 & \\ \vdots & & & & & \ddots \\ 0 & \cdots & & & & \cdots & 0 \end{bmatrix} U^T$$

The minimum norm solution is given by $x^\dagger = A^\dagger m$.

Tikhonov regularization is the classical method for noise-robust tomographic reconstruction

Write a penalty functional

$$\Phi(f) = \|Af - m\|_2^2 + \alpha\|f\|_2^2,$$

where $0 < \alpha < \infty$ is a regularization parameter. Define $\Gamma_\alpha(m)$ by

$$\Phi(\Gamma_\alpha(m)) = \min_{f \in X} \{\Phi(f)\}.$$

We denote

$$\Gamma_\alpha(m) = \arg \min_{f \in X} \{\|Af - m\|_2^2 + \alpha\|f\|_2^2\}.$$

Tikhonov regularization can be expressed as filtering the singular values of the matrix A

$$\Gamma_{\alpha}(m) = V \begin{bmatrix} \frac{d_1}{d_1^2 + \alpha} & 0 & \cdots & 0 \\ 0 & \ddots & & \vdots \\ \vdots & & \ddots & 0 \\ 0 & \cdots & 0 & \frac{d_{\min\{k,n\}}}{d_{\min\{k,n\}}^2 + \alpha} \end{bmatrix} U^T m$$

In large-scale computations it is better to use the formula

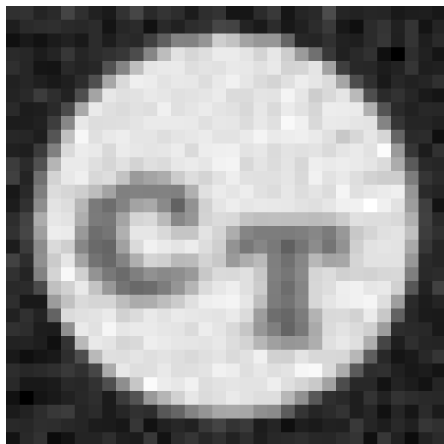
$$\Gamma_{\alpha}(m) = (A^T A + \alpha I)^{-1} A^T m.$$

Standard Tikhonov regularization

$$\arg \min_{f \in \mathbb{R}^n} \{ \|Af - m\|_2^2 + \alpha \|f\|_2^2 \}$$



Original phantom



Reconstruction

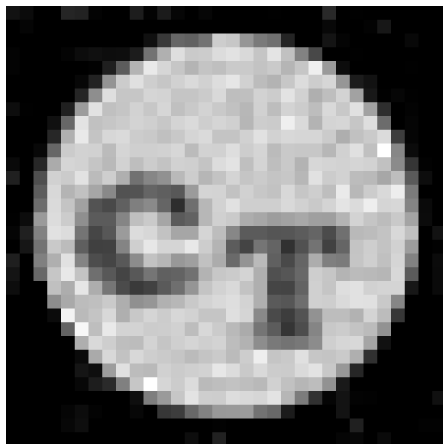
Relative square norm error 12%

Non-negative Tikhonov regularization

$$\arg \min_{f \in \mathbb{R}_+^n} \{ \|Af - m\|_2^2 + \alpha \|f\|_2^2 \}$$



Original phantom



Reconstruction

Relative square norm error 10%

Recall the L^p norms for \mathbb{R}^n

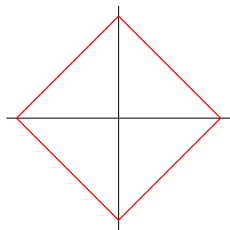
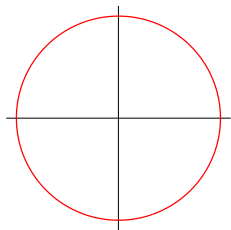
Let $f \in \mathbb{R}^n$. The L^p norms for $1 \leq p < \infty$ are defined by

$$\|f\|_p = \left(\sum_{j=1}^n |f_j|^p \right)^{1/p}.$$

In particular we use the following two cases:

$$\|f\|_2^2 = \sum_{j=1}^n |f_j|^2,$$

$$\|f\|_1 = \sum_{j=1}^n |f_j|.$$



Total variation (TV) regularization is a technique for preserving edges in the reconstruction

We consider calculating the minimizer of the TV functional

$$\begin{aligned} & \|Af - m\|_2^2 + \alpha \{ \|L_H f\|_1 + \|L_V f\|_1 \} \\ = & \|Af - m\|_2^2 + \alpha \left\{ \sum_j \sum_i \left(|f_{i(j+1)} - f_{ij}| + |f_{(i+1)j} - f_{ij}| \right) \right\} \end{aligned}$$

where L_H and L_V are horizontal and vertical first-order difference matrices. [Rudin, Osher and Fatemi 1992]

TV tomography: $\arg \min_{f \in \mathbb{R}^n} \{ \|Af - m\|_2^2 + \alpha \|\nabla f\|_1 \}$

1992 Rudin, Osher & Fatemi: denoise images by taking $A = I$

1998 Delaney & Bresler

2001 Persson, Bone & Elmqvist

2003 Kolehmainen, S, Järvenpää, Kaipio, Koistinen, Lassas, Pirttilä & Somersalo (first TV work with measured X-ray data)

2006 Kolehmainen, Vanne, S, Järvenpää, Kaipio, Lassas & Kalke

2006 Sidky, Kao & Pan

2008 Liao & Sapiro

2008 Sidky & Pan

2008 Herman & Davidi

2009 Tang, Nett & Chen

2009 Duan, Zhang, Xing, Chen & Cheng

2010 Bian, Han, Sidky, Cao, Lu, Zhou & Pan

2011 Jensen, Jørgensen, Hansen & Jensen

2011 Tian, Jia, Yuan, Pan & Jiang

2012–present: hundreds of articles indicated by Google Scholar

There are many computational approaches for computing the minimum

Primal-dual algorithms Chambolle, Chan, Chen, Esser, Golub, Mulet, Nesterov, Zhang

Thresholding Candès, Chambolle, Chaux, Combettes, Daubechies, Defrise, DeMol, Donoho, Pesquet, Starck, Teschke, Vese, Wajs

Bregman iteration Cai, Burger, Darbon, Dong, Goldfarb, Mao, Osher, Shen, Xu, Yin, Zhang

Splitting approaches Chan, Esser, Fornasier, Goldstein, Langer, Osher, Schönlieb, Setzer, Wajs

Nonlocal TV Bertozzi, Bresson, Burger, Chan, Lou, Osher, Zhang

We found that **quadratic programming** works well for us.

Quadratic programming (QP) for TV regularization

The minimizer of the functional

$$\arg \min_{f \in \mathbb{R}_+^n} \left\{ \|Af - m\|_2^2 + \alpha \|L_H f\|_1 + \alpha \|L_V f\|_1 \right\}$$

can be transformed into the standard form

$$\arg \min_{z \in \mathbb{R}^{5n}} \left\{ \frac{1}{2} z^T Q z + c^T z \right\}, \quad z \geq 0, \quad E z = b,$$

where Q is symmetric and E implements equality constraints.

Large-scale primal-dual interior point QP method was developed in Kolehmainen, Lassas, Niinimäki & S (2012) and Hämäläinen, Kallonen, Kolehmainen, Lassas, Niinimäki & S (2013).

Reduction to $\arg \min_{z \in \mathbb{R}^{5n}} \left\{ \frac{1}{2} z^T Q z + c^T z \right\}$

Denote horizontal and vertical differences by

$$L_H f = u_H^+ - u_H^- \quad \text{and} \quad L_V f = u_V^+ - u_V^-,$$

where $u_H^\pm, u_V^\pm \geq 0$. TV minimization is now

$$\arg \min_{f \in \mathbb{R}_+^n} \left\{ f^T A^T A f - 2f^T A^T m + \alpha \mathbf{1}^T (u_H^+ + u_H^- + u_V^+ + u_V^-) \right\},$$

where $\mathbf{1} \in \mathbb{R}^n$ is vector of all ones. Further, we denote

$$z = \begin{bmatrix} f \\ u_H^+ \\ u_H^- \\ u_V^+ \\ u_V^- \end{bmatrix}, \quad Q = \begin{bmatrix} \frac{1}{\sigma^2} A^T A & 0 & 0 & 0 & 0 \\ 0 & 0 & 0 & 0 & 0 \\ 0 & 0 & 0 & 0 & 0 \\ 0 & 0 & 0 & 0 & 0 \\ 0 & 0 & 0 & 0 & 0 \end{bmatrix}, \quad c = \begin{bmatrix} -2A^T m \\ \alpha \mathbf{1} \\ \alpha \mathbf{1} \\ \alpha \mathbf{1} \\ \alpha \mathbf{1} \end{bmatrix}.$$

Non-negative TV regularization

$$\arg \min_{f \in \mathbb{R}_+^n} \{ \|Af - m\|_2^2 + \alpha \|\nabla f\|_1 \}$$

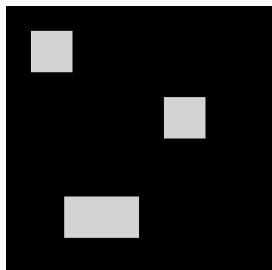


Original phantom

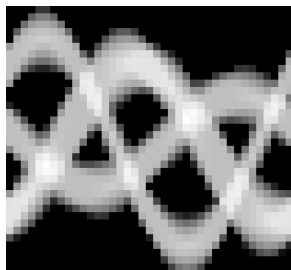
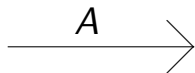


TV regularized reconstruction
Relative square norm error 7%

Recall the square phantom

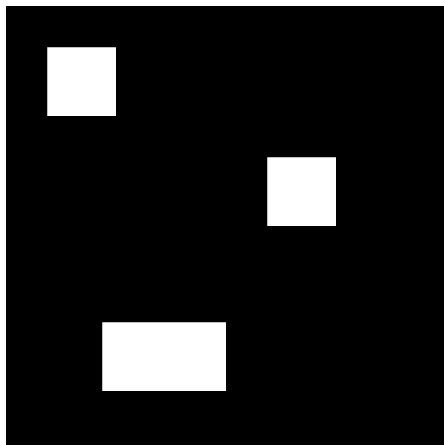


$$f \in \mathbb{R}^{32 \times 32}$$

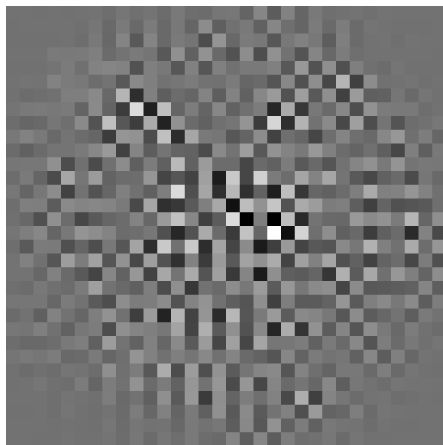


$$Af \in \mathbb{R}^{49 \times 39}$$

Naive reconstruction using the Moore-Penrose pseudoinverse; data has 0.1% relative noise



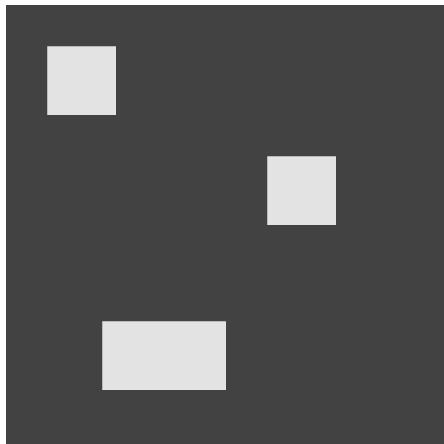
Original phantom, values between zero (black) and one (white)



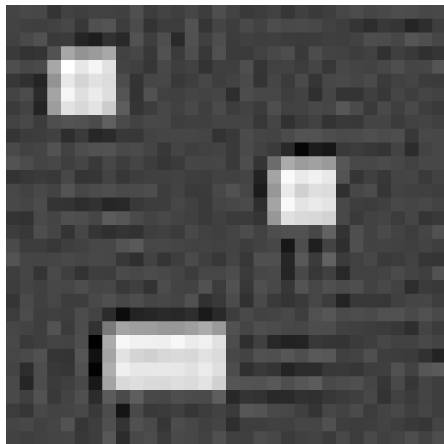
Naive reconstruction with minimum -14.9 and maximum 18.5

Standard Tikhonov regularization

$$\arg \min_{f \in \mathbb{R}^n} \{ \|Af - m\|_2^2 + \alpha \|f\|_2^2 \}$$



Original phantom

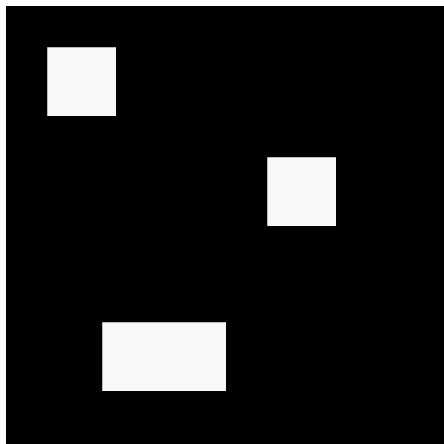


Reconstruction

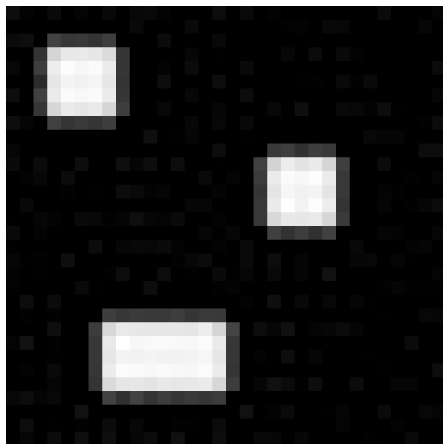
Relative square norm error 35%

Constrained Tikhonov regularization

$$\arg \min_{f \in \mathbb{R}_+^n} \{ \|Af - m\|_2^2 + \alpha \|f\|_2^2 \}$$



Original phantom

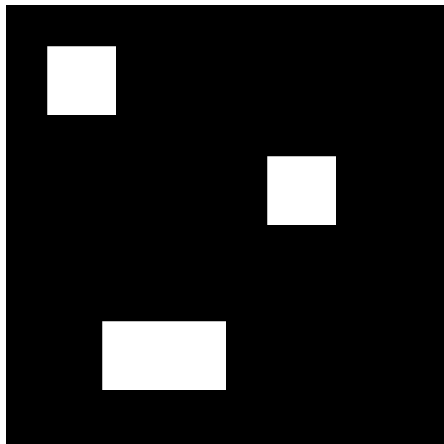


Reconstruction

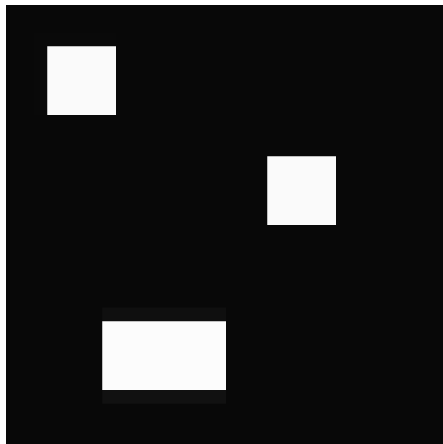
Relative square norm error 13%

Constrained total variation (TV) regularization

$$\arg \min_{f \in \mathbb{R}_+^n} \left\{ \|Af - m\|_2^2 + \alpha \left\{ \|L_H f\|_1 + \|L_V f\|_1 \right\} \right\}$$



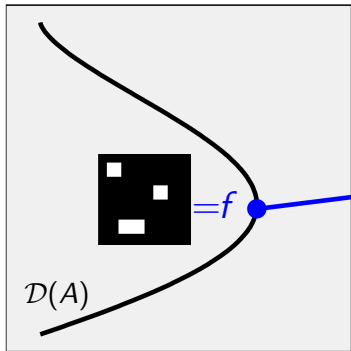
Original phantom



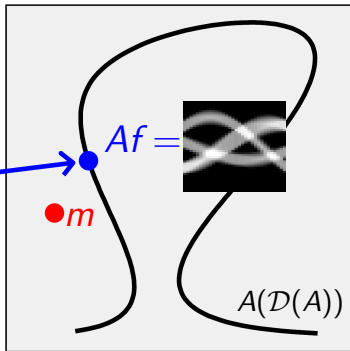
TV regularized reconstruction
Relative square norm error 3%

Inverse problem of X-ray tomography: given noisy sinogram, find a stable approximation to f

Model space $X = \mathbb{R}^{32 \times 32}$

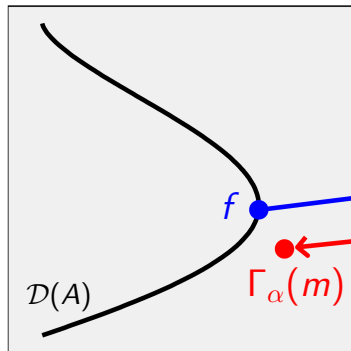


Data space $Y = \mathbb{R}^{32 \times 49}$

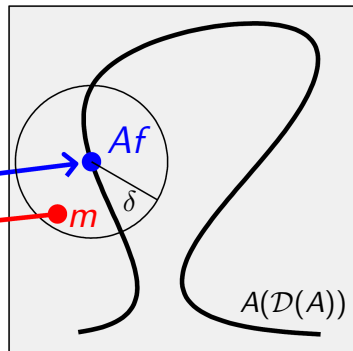


Robust solution of ill-posed inverse problems requires regularization

Model space $X = \mathbb{R}^{32 \times 32}$



Data space $Y = \mathbb{R}^{39 \times 49}$



We need to define a family of continuous functions $\Gamma_\alpha : Y \rightarrow X$ so that the reconstruction error $\|\Gamma_{\alpha(\delta)}(m) - x\|_X$ vanishes asymptotically at the zero-noise level $\delta \rightarrow 0$.

In variational regularization, the penalty term expresses *a priori* knowledge about the unknown

Standard Tikhonov regularization:

$$\arg \min_{f \in \mathbb{R}^n} \{ \|Af - m\|_2^2 + \alpha \|f\|_2^2 \}$$

Non-negativity constrained Tikhonov regularization:

$$\arg \min_{f \in \mathbb{R}_+^n} \{ \|Af - m\|_2^2 + \alpha \|f\|_2^2 \}$$

Non-negativity constrained Total Variation (TV) regularization:

$$\arg \min_{f \in \mathbb{R}_+^n} \{ \|Af - m\|_2^2 + \alpha \|\nabla f\|_1 \}$$

Outline

X-ray tomography

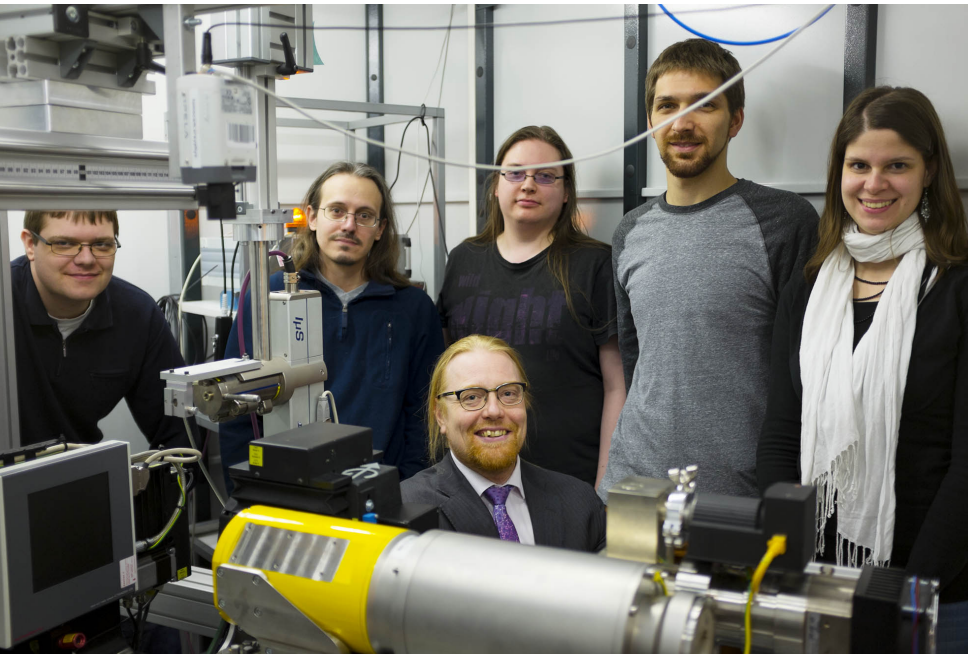
Mathematical model of X-ray attenuation

Tomography with few data: ill-posed inverse problem

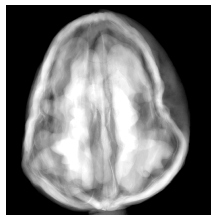
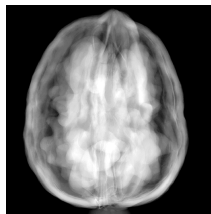
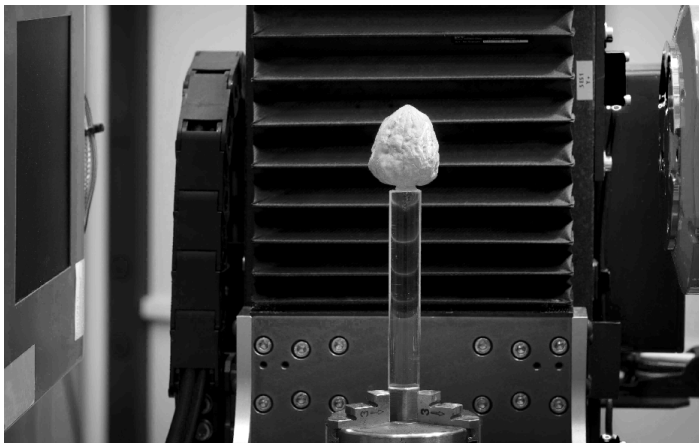
Regularized inversion

A real-world example

This is Professor Keijo Hämäläinen's X-ray lab



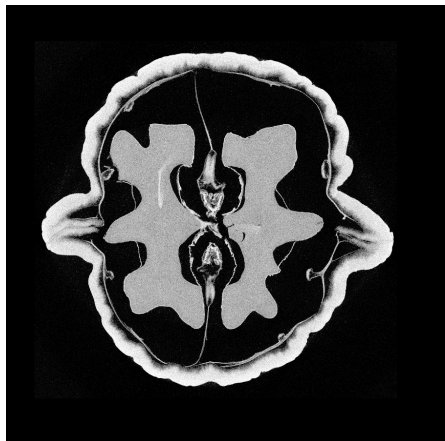
We collected X-ray projection data of a walnut from 1200 directions



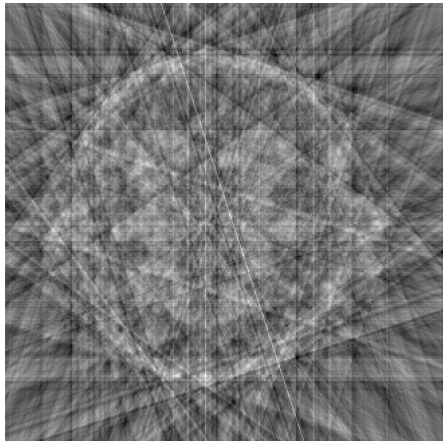
Laboratory and data collection by Keijo Hämäläinen and Aki Kallonen, University of Helsinki.

The data is openly available at <http://fips.fi/dataset.php>, thanks to Esa Niemi and Antti Kujanpää

Reconstructions of a 2D slice through the walnut using filtered back-projection (FBP)

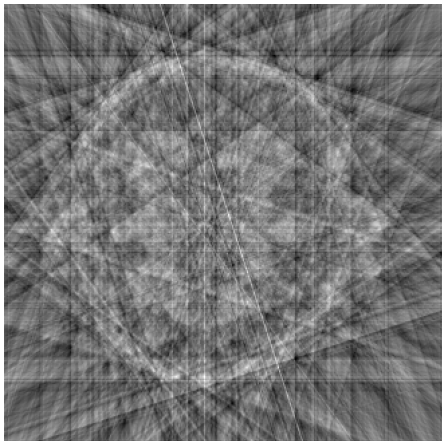


FBP with comprehensive data
(1200 projections)

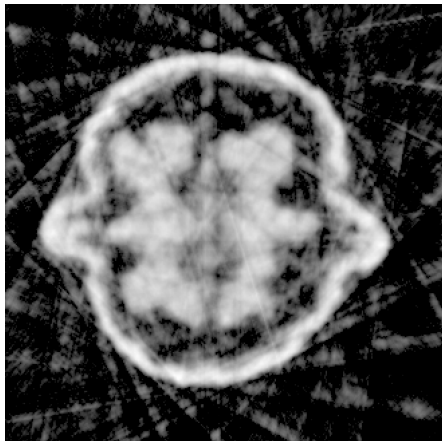


FBP with sparse data
(20 projections)

Sparse-data reconstruction of the walnut using non-negative Tikhonov regularization



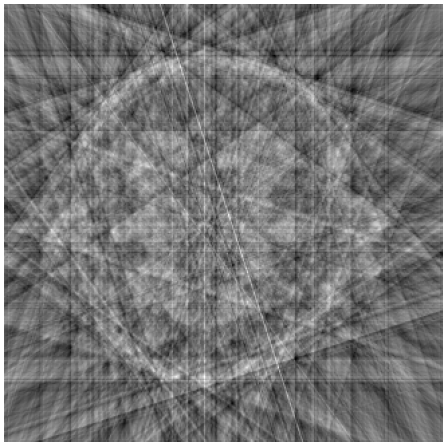
Filtered back-projection



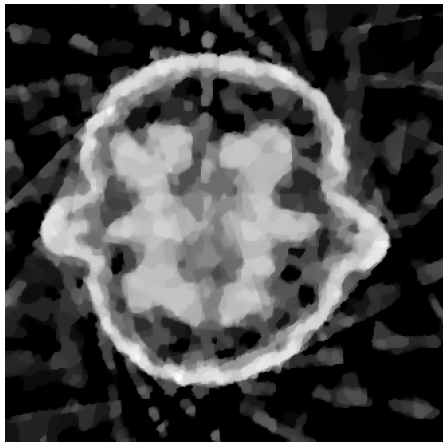
Constrained Tikhonov regularization

$$\arg \min_{f \in \mathbb{R}_+^n} \{ \|Af - m\|_2^2 + \alpha \|f\|_2^2 \}$$

Sparse-data reconstruction of the walnut using non-negative total variation regularization

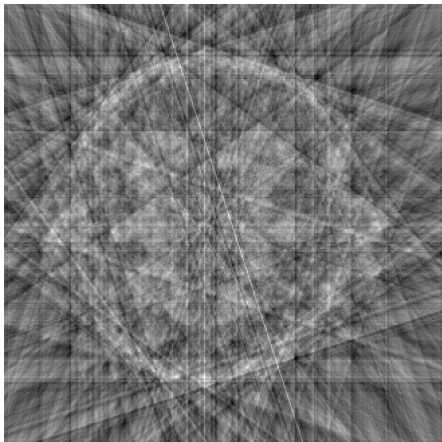


Filtered back-projection

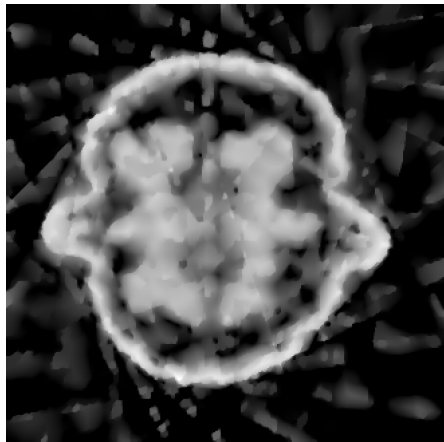


Constrained TV regularization
$$\arg \min_{f \in \mathbb{R}_+^n} \{ \|Af - m\|_2^2 + \alpha \|\nabla f\|_1 \}$$

Sparse-data reconstruction of the walnut using Total Generalized Variation (TGV)



Filtered back-projection



TGV: thanks to Kristian Bredies!

Daubechies, Defrise and de Mol introduced a revolutionary method in 2004

The sparsity-promoting iteration works like this:

$$f_n = \mathcal{S}_\mu(f_{n-1} + A^T(m - Af_{n-1})),$$

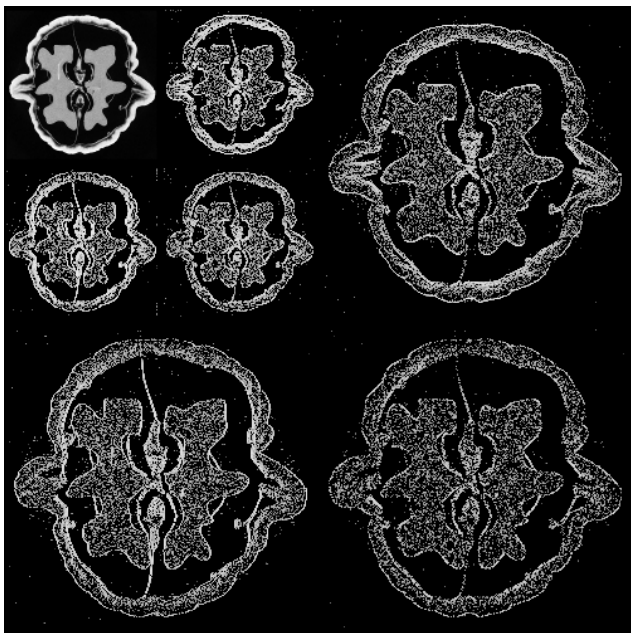
where the soft-thresholding operator \mathcal{S}_μ is defined by

$$\mathcal{S}_\mu(g) = \sum_{j \in J} \mathcal{S}_\mu(\langle g, \psi_j \rangle) \psi_j(x).$$

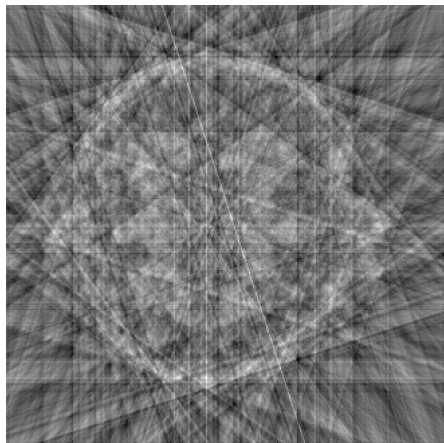
Here ψ_j are for example wavelets or shearlets, forming a frame, and

$$\mathcal{S}_\mu(x) = \begin{cases} x + \frac{\mu}{2} & \text{if } x \leq -\frac{\mu}{2} \\ 0 & \text{if } |x| < \frac{\mu}{2} \\ x - \frac{\mu}{2} & \text{if } x \geq \frac{\mu}{2}. \end{cases}$$

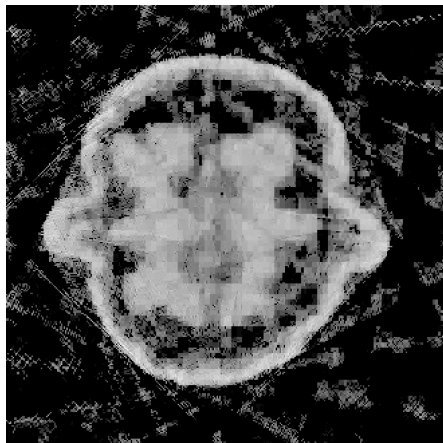
Illustration of the Haar wavelet transform



Sparse-data reconstruction of the walnut using Haar wavelet sparsity

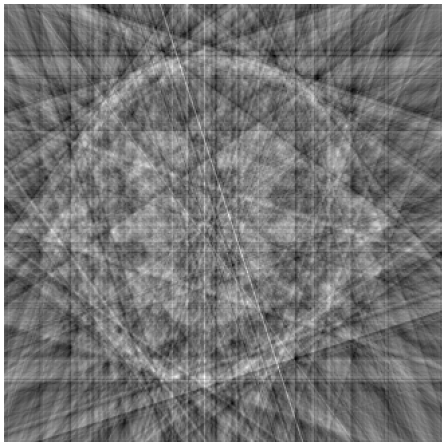


Filtered back-projection

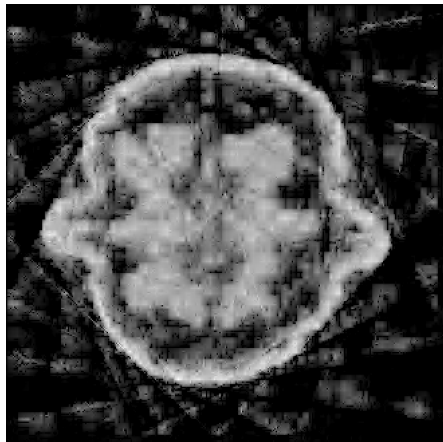


Constrained Besov regularization
$$\arg \min_{f \in \mathbb{R}_+^n} \left\{ \|Af - m\|_2^2 + \alpha \|f\|_{B_{11}^1} \right\}$$

Sparse-data reconstruction of the walnut using Daubechies 2 wavelet sparsity

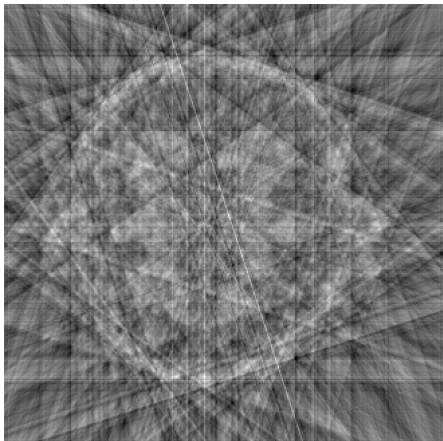


Filtered back-projection

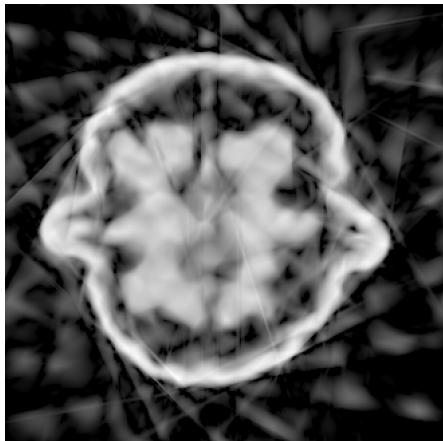


Constrained Besov regularization
$$\arg \min_{f \in \mathbb{R}_+^n} \left\{ \|Af - m\|_2^2 + \alpha \|f\|_{B_{11}^1} \right\}$$

Sparse-data reconstruction of the walnut using shearlet sparsity

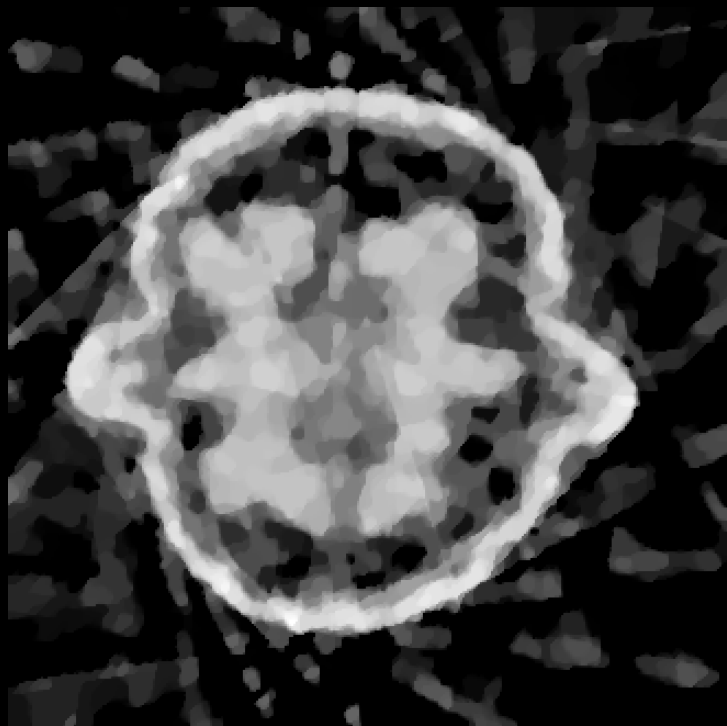


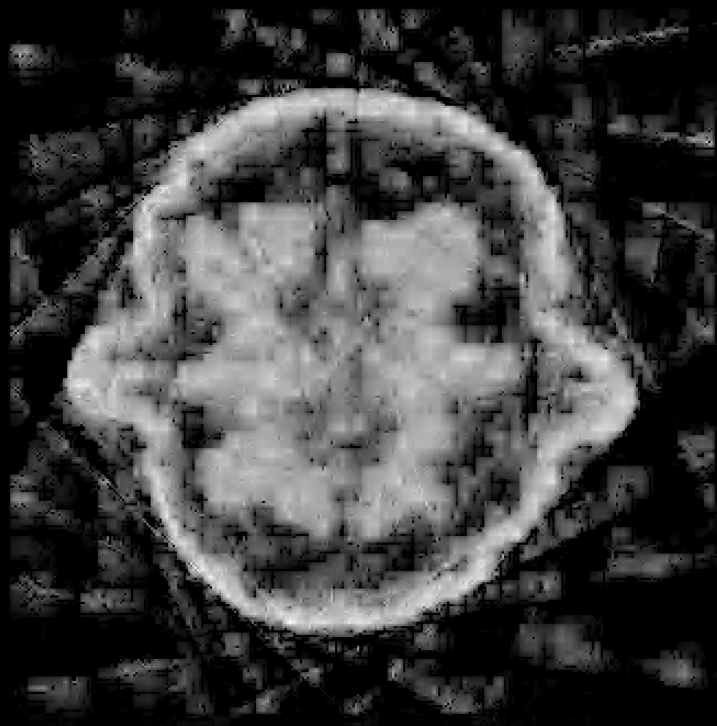
Filtered back-projection

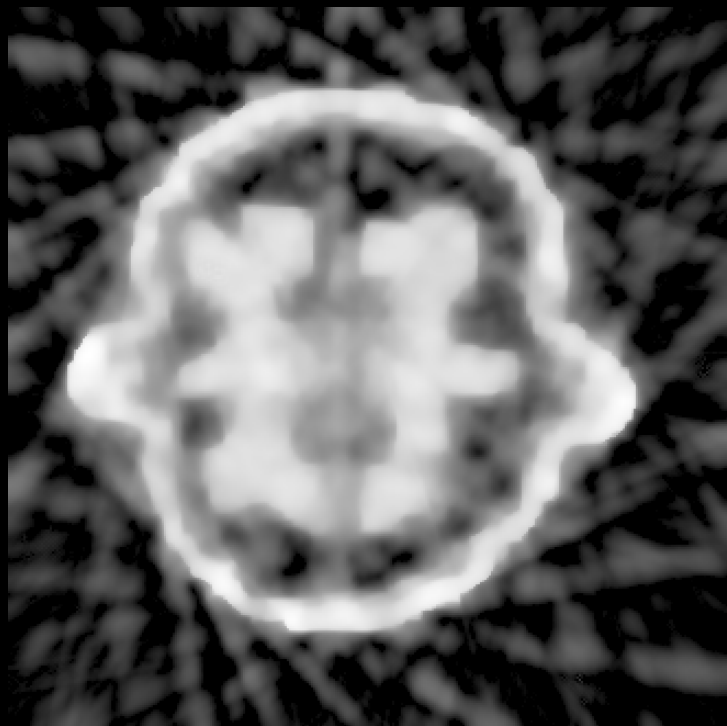


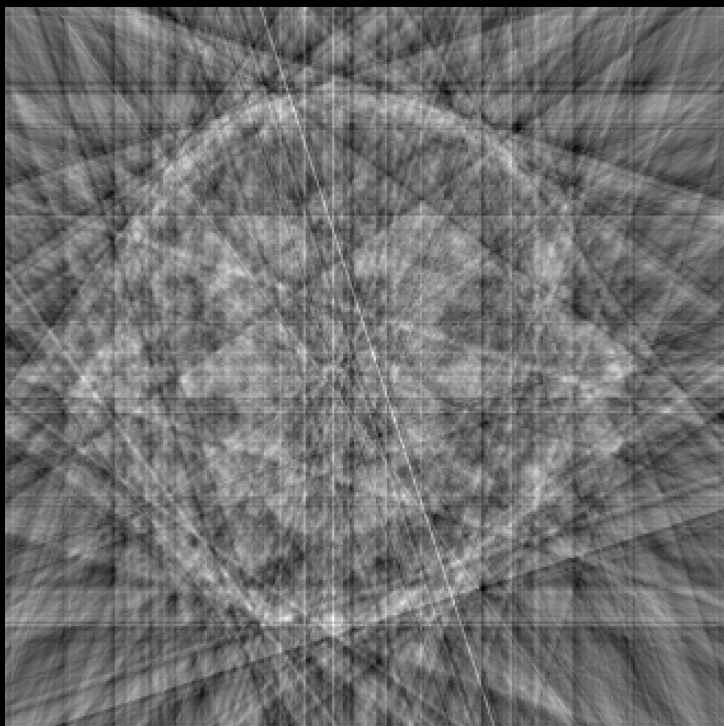
Thanks to Gitta Kutyniok!
<http://www.shearlab.org/>

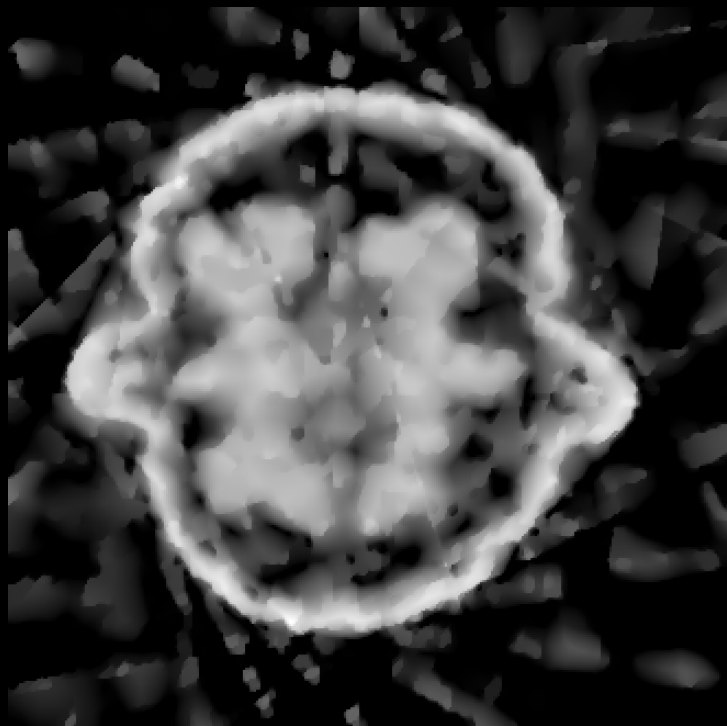


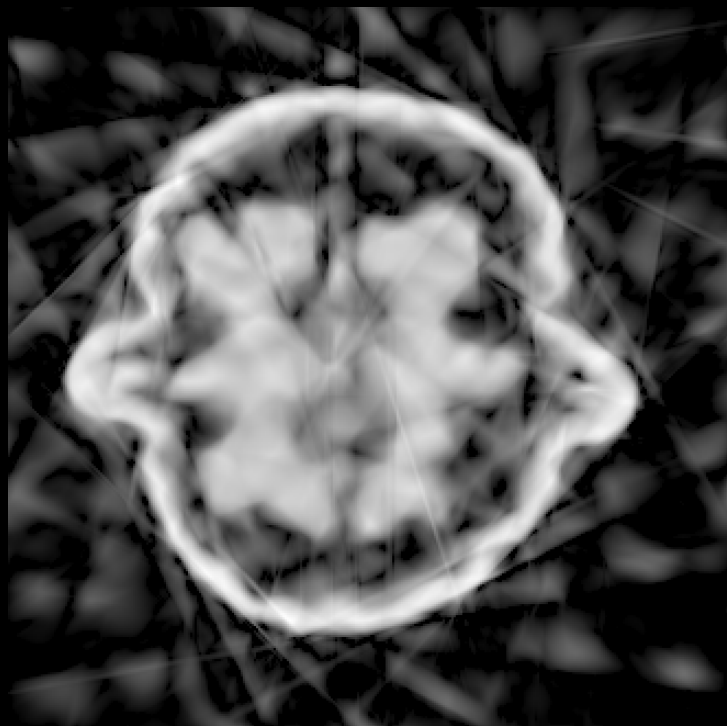




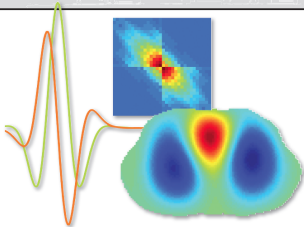








JENNIFER L. MUELLER • SAMULI SILTANEN



Linear and Nonlinear
Inverse Problems with
Practical Applications

Computational Science & Engineering **siam**

All Matlab codes freely
available at this site!

Part I: Linear Inverse Problems

- 1 Introduction
- 2 Naïve reconstructions and inverse crimes
- 3 Ill-Posedness in Inverse Problems
- 4 Truncated singular value decomposition
- 5 Tikhonov regularization
- 6 Total variation regularization
- 7 Besov space regularization using wavelets
- 8 Discretization-invariance
- 9 Practical X-ray tomography with limited data
- 10 Projects

Part II: Nonlinear Inverse Problems

- 11 Nonlinear inversion
- 12 Electrical impedance tomography
- 13 Simulation of noisy EIT data
- 14 Complex geometrical optics solutions
- 15 A regularized D-bar method for direct EIT
- 16 Other direct solution methods for EIT
- 17 Projects

Finnish Inverse Problems Society offers open X-ray tomographic datasets



See the website <https://www.fips.fi/dataset.php>

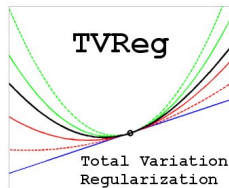
The ASTRA toolbox contains important algorithms

See the website <http://www.astra-toolbox.com/>

[W. van Aarle, W. J. Palenstijn, J. Cant, E. Janssens, F. Bleichrodt, A. Dabravolski, J. De Beenhouwer, K. J. Batenburg, and J. Sijbers 2016]

[W. van Aarle, W. J. Palenstijn, J. De Beenhouwer, T. Altantzis, S. Bals, K. J. Batenburg, and J. Sijbers 2015]

Another great resource is Per Christian Hansen's 3D tomography toolbox TVreg



TVreg: Software for 3D Total Variation Regularization (for Matlab Version 7.5 or later), developed by Tobias Lindstrøm Jensen, Jakob Heide Jørgensen, Per Christian Hansen, and Søren Holdt Jensen.

Website: <http://www2.imm.dtu.dk/~pcha/TVReg/>

These books are recommended for learning the mathematics of practical X-ray tomography

1983 Deans: The Radon Transform and Some of Its Applications

1986 Natterer: The mathematics of computerized tomography

1988 Kak & Slaney: Principles of computerized tomographic imaging

1996 Engl, Hanke & Neubauer: Regularization of inverse problems

1998 Hansen: Rank-deficient and discrete ill-posed problems

2001 Natterer & Wübbeling: Mathematical Methods in Image Reconstruction

2008 Buzug: Computed Tomography: From Photon Statistics to Modern Cone-Beam CT

2008 Epstein: Introduction to the mathematics of medical imaging

2010 Hansen: Discrete inverse problems

2012 Mueller & S: Linear and Nonlinear Inverse Problems with Practical Applications

2014 Kuchment: The Radon Transform and Medical Imaging



Thank you for your attention!